



DNA damage response in renal ischemia–reperfusion and ATP-depletion injury of renal tubular cells



Zhengwei Ma^a, Qingqing Wei^a, Guie Dong^a, Yuqing Huo^b, Zheng Dong^{a,c,*}

^a Department of Cellular Biology and Anatomy, Medical College of Georgia, Georgia Regents University and Charlie Norwood VA Medical Center, Augusta, GA 30912, USA

^b Vascular Biology Center, Medical College of Georgia, Georgia Regents University and Charlie Norwood VA Medical Center, Augusta, GA 30912, USA

^c Department of Nephrology, The Second Xiangya Hospital, Central South University, Changsha, China

ARTICLE INFO

Article history:

Received 13 January 2014

Received in revised form 25 March 2014

Accepted 2 April 2014

Available online 12 April 2014

Keywords:

Renal ischemia–reperfusion

Acute kidney injury

ATP depletion

DNA damage response

Apoptosis

ABSTRACT

Renal ischemia–reperfusion leads to acute kidney injury (AKI) that is characterized pathologically by tubular damage and cell death, followed by tubular repair, atrophy and interstitial fibrosis. Recent work suggested the possible presence of DNA damage response (DDR) in AKI. However, the evidence is sketchy and the role and regulation of DDR in ischemic AKI remain elusive. In this study, we demonstrated the induction of phosphorylation of ATM, H2AX, Chk2 and p53 during renal ischemia–reperfusion in mice, suggesting DDR in kidney tissues. DDR was also induced in vitro during the recovery or “reperfusion” of renal proximal tubular cells (RPTCs) after ATP depletion. DDR in RPTCs was abrogated by supplying glucose to maintain ATP via glycolysis, indicating that the DDR depends on ATP depletion. The DDR was also suppressed by the general caspase inhibitor z-VAD and the overexpression of Bcl-2, supporting a role of apoptosis-associated DNA damage in the DDR. N-acetylcysteine (NAC), an antioxidant, suppressed the phosphorylation of ATM and p53 and, to a less extent, Chk2, but NAC increased the phosphorylation and nuclear foci formation of H2AX. Interestingly, NAC increased apoptosis, which may account for the observed H2AX activation. Ku55933, an ATM inhibitor, blocked ATM phosphorylation and ameliorated the phosphorylation of Chk2 and p53, but it increased H2AX phosphorylation and nuclear foci formation. Ku55933 also increased apoptosis in RPTCs following ATP depletion. The results suggest that DDR occurs during renal ischemia–reperfusion in vivo and ATP-depletion injury in vitro. The DDR is partially induced by apoptosis and oxidative stress-related DNA damage. ATM, as a sensor in the DDR, may play a cytoprotective role against tubular cell injury and death.

© 2014 Elsevier B.V. All rights reserved.

1. Introduction

Renal ischemia–reperfusion is a major cause of acute kidney injury (AKI), which leads to high mortality in patients and may progress to chronic kidney disease. Pathologically, ischemic AKI is characterized by sublethal and lethal damages in renal tubules, especially the proximal tubules [1,2]. Cell death in renal tubules in the forms of both apoptosis and necrosis is detected in animal models as well as the kidneys of AKI patients. Interestingly, renal tubules possess the capacity of repair and when the repair is incomplete, fibrosis or “scar” develops, contributing to gradual loss of renal function and chronic deficiency [3,4]. The molecular basis of tubular cell death and repair remains poorly understood.

DNA damage occurs in a variety of conditions such as irradiation, UV exposure, genotoxic chemical challenge, and oxidative stress or free

radical insult. In response to DNA damage, cells activate a network of signaling pathways known as DNA damage response (DDR). DDR starts from the activation of the ‘sensor’ protein kinases, including the phosphoinositol 3-kinase-like serine/threonine protein kinases ataxia telangiectasia mutated (ATM), ATM- and Rad3-related (ATR), and DNA-dependent protein kinase (DNA-PK). The ‘sensor’ kinases relay the signal to the ‘executors’ kinases, especially Check-point kinases (Chk1 and Chk2), which then phosphorylate a multitude of proteins to induce cell cycle arrest or, in the presence of severe DNA damage, cell death [5–7].

DNA damage, such as the accumulation of 8-oxo-dG and apoptosis-associated DNA cleavage in renal tubular cells, is known to occur in kidney tissues following ischemia–reperfusion [8–10]. In experimental models of renal ischemia–reperfusion, p53 is activated and inhibition of p53 provides renoprotective effects, implying the possibility of DDR [11,12]. However, DDR has not been studied in kidney cells or tissues during renal ischemia–reperfusion. In cisplatin-induced AKI, we have delineated a DDR signaling pathway that involves the activation of ATR followed by Chk2 activation and the phosphorylation of p53,

* Corresponding author at: Department of Nephrology, The Second Xiangya Hospital, Central South University, Changsha, Hunan, China. Tel.: +1 706 721 2825.

E-mail address: zdong@gru.edu (Z. Dong).

leading to the expression of apoptotic genes, such as PUMA- α , to result in tubular cell death [13–15]. Whether DDR occurs in renal ischemia–reperfusion and what role it plays in kidney injury and repair remain largely unknown.

In the present study, we detected DDR in kidney tissues during ischemia–reperfusion in mice and in ATP-depleted renal tubular cells. The DDR was suppressed to various extents by the ATM inhibitor Ku55933, the antioxidant N-acetylcysteine, the general caspase inhibitor z-VAD and overexpression of Bcl-2. It is suggested that DDR occurs in ischemic AKI via multiple mechanisms, including apoptotic DNA fragmentation and oxidative stress.

2. Materials and methods

2.1. Reagents and antibodies

Antibodies were from the following sources: anti-Chk1 from Epitomics (Burlingame, CA); anti-Chk2, Anti-p53, anti- γ H2AX, anti-PARP and anti-phosphorylated Chk1 (serine 345) from Cell Signaling Technology (Beverly, MA), anti-phosphorylated Chk2 (Threonine-68) from Novus (Littleton, CO), anti-ATM antibody from Abcam (Cambridge, MA), anti-phosphorylated ATM (serine-1981) from Millipore (Billerica, MA); anti- β -actin from Sigma (St. Louis, MO); all secondary antibodies from Jackson ImmunoResearch (West Grove, PA). Ku55933 was purchased from Selleck (Houston, TX). Other reagents and chemicals including azide were purchased from Sigma (St. Louis, MO).

2.2. Renal ischemia–reperfusion

Male mice of 8 to 10 week old C57BL/6 mice were purchased from Jackson Laboratory (Bar Harbor, MN) and maintained in the animal facility of Charlie Norwood VA Medical Center under a 12-hour light/12-hour dark pattern with free access to food and water. All animal experiments were performed according to a protocol approved by the Institutional Animal Care and Use Committee of Charlie Norwood VA Medical Center. Renal ischemia–reperfusion was induced as detailed recently [16]. Briefly, after anesthetization with pentobarbital (50 mg/kg, i.p.), the mice were kept on a Homoeothermic Blanket Control Unit (Harvard Apparatus Ltd, UK) with a rectal probe to monitor and maintain the body temperature at 36.4 °C. Flank incisions were made to expose both renal pedicles for bilateral clamping to induce 30 min of renal ischemia. The clamps were then released for reperfusion. Kidneys were collected after 48 h of reperfusion for the following examinations. Color changes of kidneys during the initiation of clamping and after removal of clamps were observed to monitor the renal ischemia and reperfusion. Control animals were subjected to sham operation without renal pedicle clamping. Renal function was monitored by measuring BUN and serum creatinine using analytical kits from Biotron Diagnostics (Hemet, CA) and Stanbio Laboratory (Boerne, TX), respectively.

2.3. Immunohistochemistry

Kidneys were collected and fixed in 4% paraformaldehyde, paraffin embedded, and sectioned at 4 μ m. The tissue sections were then deparaffinized and rehydrated, Antigen retrieval was conducted by 1 h of incubation at 95 °C in 0.01 M sodium citrate, pH 6.0. The tissues were subsequently incubated with 3% H₂O₂ at 37 °C for 30 min to block the endogenous peroxidase activity. Then, the tissues were incubated sequentially with a blocking buffer (2% BSA, 0.2% nonfat dry milk, 0.8% Triton X-100, and 2% normal donkey serum) and the anti- γ H2AX antibody (1:250 dilution, Cell Signaling, Danvers, USA) in the blocking buffer. After incubation with biotin-labeled secondary antibody, the color was developed with an ABC kit from Vector Laboratories (Burlingame, CA). The staining was evaluated in a blinded manner.

2.4. Cell ATP depletion and recovery

The rat kidney proximal tubular cell line (RPTC) was originally obtained from Dr. U. Hopfer (Case Western Reserve Univ., Cleveland, OH) and cultured in serum-supplemented Ham's F-12/Dulbecco's modified Eagle's medium with 17.5 mM glucose as described previously [17, 18]. Stable Bcl-2-overexpressing RPTC were generated as described before [18]. For the experiment, the cells were seeded in 35 mm collagen-coated dishes. After overnight growth, the cells were washed with phosphate-buffered saline and subjected to ATP depletion by incubation in glucose-free Krebs–Ringer bicarbonate buffer containing 10 mM azide. Following ATP depletion, the cells were incubated in full culture medium without azide for recovery or 'reperfusion'.

2.5. Apoptosis evaluation

Cells were fixed with 4% paraformaldehyde and the nuclei were stained by Hoechst 33342. The apoptotic cells were identified by the apoptotic morphology under phase contrast microscope and the condensed nuclei under fluorescent microscope.

2.6. Immunoblot analysis

A standard protocol of immunoblot analysis was followed. Briefly, the protein concentration of cell lysate was determined by using the BCA reagent (Pierce, Rockford, IL). Equal amounts of proteins (20 μ g) were loaded for reducing SDS-gel electrophoresis, followed by transferring onto polyvinylidene difluoride membranes. The blots were then incubated sequentially in blocking buffer, primary antibody, and the horseradish peroxidase-conjugated secondary antibody. Finally, the antigens on the blots were revealed using the enhanced chemiluminescence kit from Pierce. All primary antibodies were used at 1:1000 dilutions for immunoblot analysis.

2.7. Immunofluorescence

Cells were grown on glass coverslips for indirect immunofluorescence as described previously [13]. Briefly, the cells were fixed with 4% paraformaldehyde and permeabilized with 0.4% Triton X-100 in a blocking buffer. The cells were then exposed to primary antibodies, followed by incubation with Cy3-labeled donkey anti-rabbit secondary antibodies. The nuclei were counter-stained by Hoechst 33342. After washes, the coverslips were mounted on slides with Antifade (Life Technologies, Grand Island, NY) for examination by confocal microscopy using Cy3 and DAPI channels.

2.8. MTT assay

After azide treatment, the cells were recovered for 24 h in full culture medium to determine cell viability using MTT assay kit according to the manufacturer's instruction (Molecular Probes, Eugene, OR).

2.9. Statistics

All data were analyzed by Microsoft Excel 2010 or SPSS. Student *t*-test or One-way ANOVA analysis was used for statistics and *P* < 0.05 was considered as significantly different.

3. Results

3.1. DDR is induced in kidney tissues during renal ischemia–reperfusion

We used a commonly used mouse model of renal ischemia–reperfusion to examine DDR in the kidney tissues. As shown in Fig. 1A, 30 min of bilateral renal ischemia followed by 48 h of reperfusion induced the loss of renal function as indicated by significant increases in

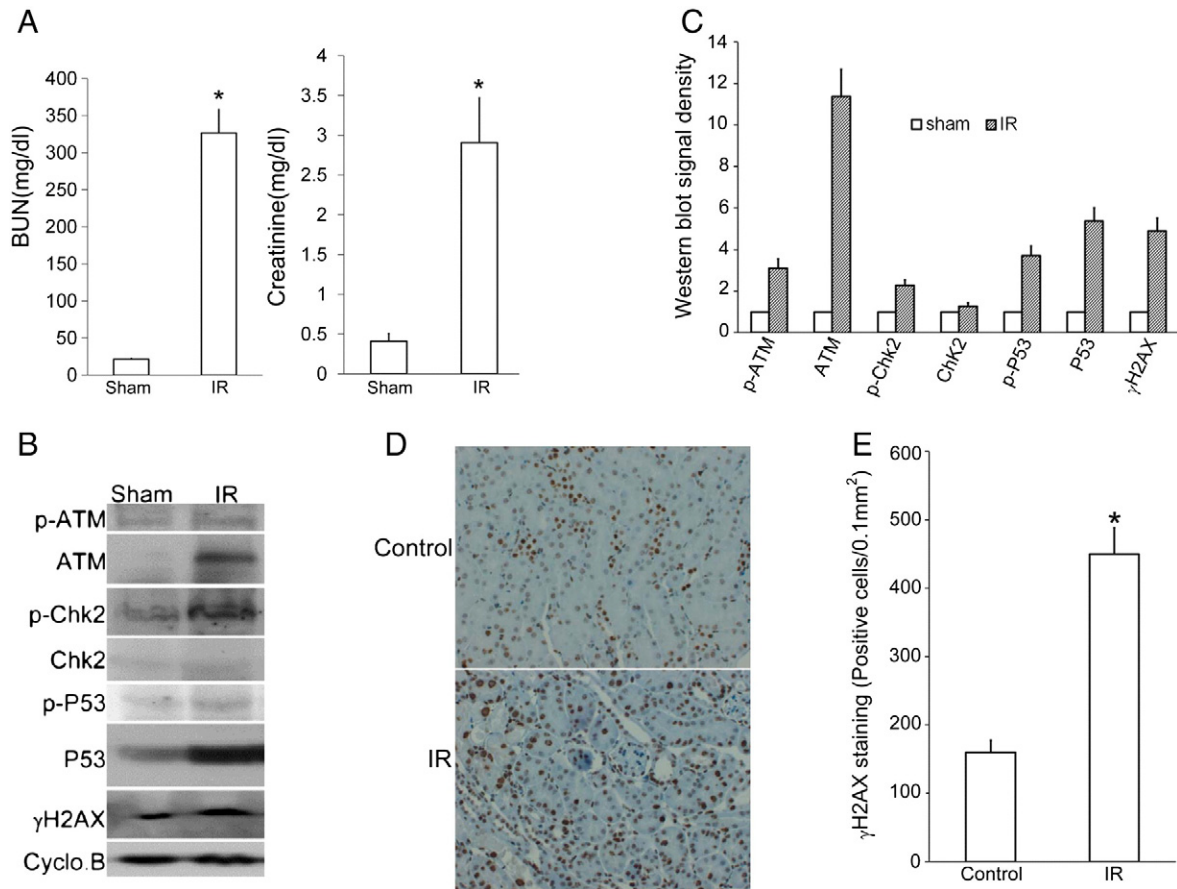


Fig. 1. DDR is induced in kidney tissues during ischemia–reperfusion in mice. C57BL/6 male mice were subjected to sham operation or 30 min of bilateral renal ischemia, followed by 48 h of reperfusion. (A) Blood samples were collected for the measurement of blood urea nitrogen and serum creatinine. Data are presented as mean \pm SD ($n = 7$); *, $p < 0.05$ vs. sham control. (B) Kidney cortex and outer medulla tissue were collected for immunoblot analysis of phosphorylated (Serine 1981) ATM, total ATM, phosphorylated (threonine 68) Chk2, total Chk2, phosphorylated (Serine 15) p53, total p53, phosphorylated H2AX (γ H2AX), and cyclophilin B as the protein loading control. (C) Quantitative analysis of the ratio of phosphorylated (Serine 1981) ATM, total ATM, phosphorylated (threonine 68) Chk2, total Chk2, phosphorylated (Serine 15) p53, total p53, phosphorylated H2AX (γ H2AX) to Cyclophilin B. Data are mean \pm SD ($n = 3$). (D) Representative images of immunohistochemistry staining of γ H2AX in kidney cortex. It demonstrates that γ H2AX is expressed in the nuclei. (E) Quantitative analysis of γ H2AX-positive tubular epithelial cells in Fig.(1D). γ H2AX-positive cells were quantified by cell counting in comparable regions of the tissues. Data are shown as means \pm SD ($n = 5$). *, $P < 0.05$ vs. Sham control.

blood urea nitrogen (BUN) and serum creatinine (Fig. 1A). To analyze DDR, we first examined the expression of ATM, a DNA damage sensor that is rapidly recruited to the double strand breaks by the Mre11–Rad50–Nbs1 complex to phosphorylate the downstream ‘effector’ protein kinases including Chk2 [19–21]. As shown in Fig. 1B and C, ATM expression was barely detectable in control tissues, but it was induced dramatically in mouse kidney tissues after ischemia–reperfusion. ATM phosphorylation at Ser1981 was also moderately induced by renal ischemia–reperfusion. Correlatively, Chk2 phosphorylation was increased, which was accompanied with increases in both total and phosphorylated p53 (ser-15) (Fig. 1B). In mammalian cells, histone H2AX phosphorylation at ser139 by ATM is a biochemical hallmark of DDR. Phosphorylated H2AX, also called γ H2AX, accumulates at the DNA damage site to recruit DNA repair complex to form nuclei foci [22,23]. γ H2AX was low in sham operated kidneys and was induced following ischemia–reperfusion. γ H2AX positive tubular epithelial cells were significantly increased in ischemia–reperfusion cortex tissues compared to the sham control (Fig. 1D, E), further implying the induction of DDR following ischemia–reperfusion. Together, these results indicate the induction of DDR during renal ischemia–reperfusion.

3.2. DDR is induced in RPTCs following azide-induced ATP depletion injury

To study the mechanism of DDR in renal ischemia–reperfusion, we used an in vitro model of ‘chemical hypoxia’, in which RPTCs were

incubated with azide (an inhibitor of respiratory complex IV) in a glucose-free buffer to induced ATP depletion. After ATP depletion, the cells were returned to full culture medium for recovery to mimic reperfusion. This in vitro model was used to investigate cell injury in renal ischemia–reperfusion in our recent studies [17,24,25]. γ H2AX was not detected in control cells and was not induced during ATP depletion (Fig. 2A: lanes 1, 2). However, after ATP-depleted cells were returned to full culture medium for recovery or ‘reperfusion’, γ H2AX was induced at 1 h, reached a higher level at 3 h and remained to be elevated after 20 h (Fig. 2A: lanes 3–5). Immunofluorescence showed weak, diffuse signals of γ H2AX in the nuclei of most control cells. However, after ATP depletion and recovery, γ H2AX accumulated to form nuclear foci (Fig. 2B). Interestingly, a significant population of the γ H2AX positive nuclei was not apoptotic as indicated by double staining with DAPI (Fig. 2C). The phosphorylation of ATM, Chk2 and p53 was increased during recovery of ATP-depleted cells (Fig. 2 D, E: lanes 3, 4), further confirming the induction of DDR in this in vitro model.

3.3. Glucose added during azide treatment prevents DDR

What triggers DDR during the recovery of ATP-depleted RPTCs? With this question, we first determined if the DDR is related to ATP depletion. Previous work demonstrated that glucose provided during mitochondrial inhibition enables cellular ATP production via glycolysis [18]. Thus we examined the effect of glucose added during azide

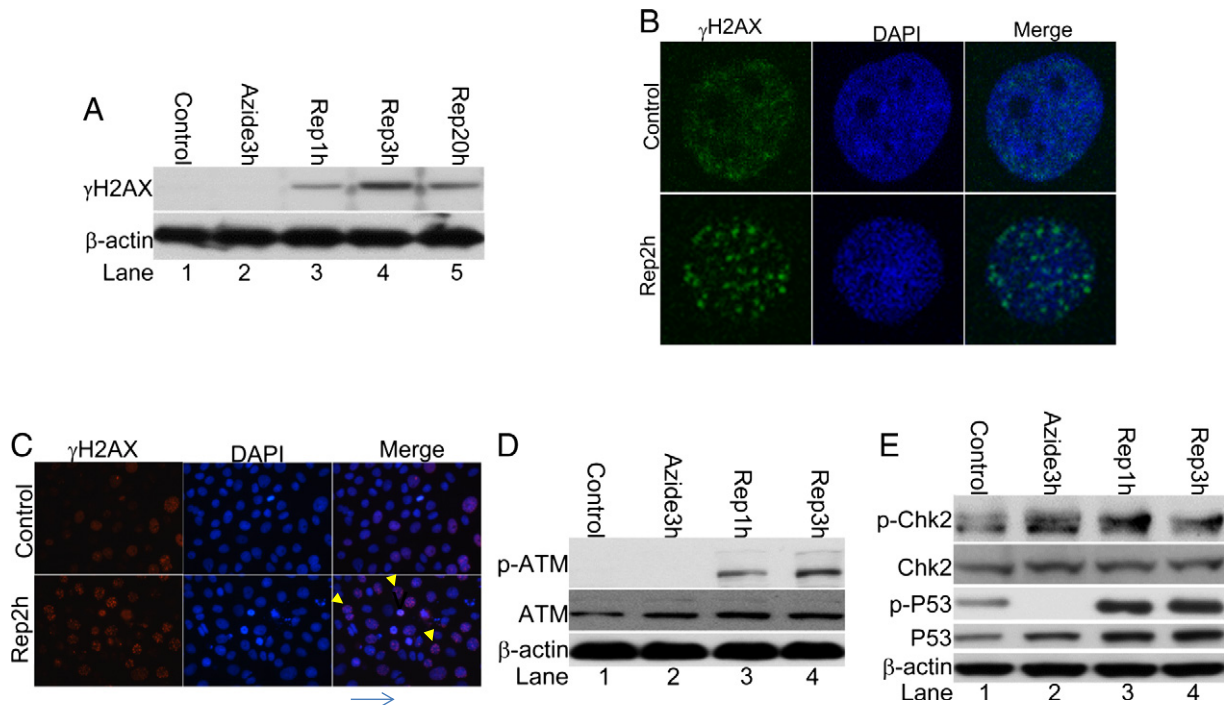


Fig. 2. DDR is induced following ATP-depletion injury in RPTC. RPTC cells were left untreated (control) or treated with 10 mM sodium azide for 3 h, followed by recovery in full medium for 0, 1, 2, 3 or 20 h as indicated. (A) Whole cell lysate was collected for immunoblot analysis of phosphorylated H2AX (γ H2AX), and β -actin (sample loading control); (B, C) The cells were fixed and subjected to immunofluorescence staining of phosphorylated H2AX (γ H2AX). (D) Whole cell lysate was collected for immunoblot analysis of phosphorylated (Serine 1981) ATM, total ATM and β -actin. (E) Whole cell lysate was collected for immunoblot analysis of phosphorylated (threonine 68) Chk2, total Chk2, phosphorylated (Ser15) p53, total p53, and β -actin.

treatment. As shown in Fig. 3, the addition of 5 and 10 mM glucose during azide treatment attenuated the induction of γ H2AX and the phosphorylation of ATM at 1 and 3 h of recovery (lanes 4, 5 vs. 3, lanes 7, 8 vs. 6), indicating that DDR in this model is causally related to the initial ATP depletion.

3.4. Inhibition of DDR following azide treatment by Z-VAD and Bcl-2

We showed previously that renal ischemia–reperfusion and ATP depletion in RPTCs activate the mitochondrial pathway of apoptosis [17, 24,26]. Since apoptosis is associated with extensive internucleosomal DNA cleavage, we reasoned that the DDR observed during the recovery period of ATP-depleted cells may be partly attributable to apoptosis. To test this possibility, the pan-caspase inhibitor Z-VAD was added during

ATP depletion and the subsequent recovery to suppress apoptosis. As expected, 50 and 100 μ M Z-VAD blocked the cleavage of caspase 3 and PARP, a biochemical hallmark of apoptosis, during azide treatment and 3 h of recovery (Fig. 4A: lanes 4, 5 vs. 3). Notably, Z-VAD also attenuated γ H2AX expression, while the phosphorylation of ATM, Chk2, and p53 was only marginally inhibited by Z-VAD (Fig. 4A: lanes 4, 5 vs. 3).

We further examined the effect of overexpression of Bcl-2, a well-known anti-apoptotic gene. As shown in Fig. 4B (lanes 7, 8 vs. 3, 4), Bcl-2 overexpression totally blocked γ H2AX induction and significantly blocked ATM, Chk2 and p53 phosphorylation. As shown previously [17, 26], azide-induced apoptosis was markedly suppressed in Bcl-2-overexpressing cells (Fig. 4C). Together, these results suggest that apoptosis-associated DNA cleavage contributes significantly to the DDR observed in this ATP-depletion/recovery model.

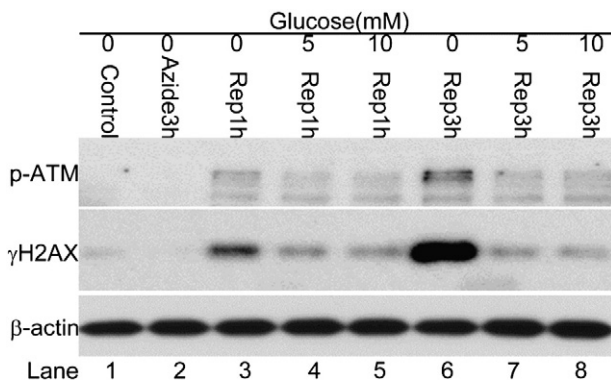


Fig. 3. Glucose added during azide treatment prevents DDR. RPTC cells were left untreated (control) or treated with 10 mM sodium azide for 3 h in the presence or absence of 5 or 10 mM D-Glucose, followed by recovery in full medium for 0, 1, or 3 h. Whole cell lysate was collected for immunoblot analysis of phosphorylated (Serine 1981) ATM and phosphorylated H2AX (γ H2AX). β -actin was used as a loading control.

3.5. N-acetylcysteine suppresses ATM activation during recovery of ATP-depleted cells

Mitochondria are an important source for reactive oxygen species (ROS) generation inside the cells [27]. The generation of ROS in the form of superoxide anion is only 3 to 5% of total oxygen consumed during normal oxidative phosphorylation [28]. However, under conditions when oxidative phosphorylation is inhibited, this rate of ROS production can be increased greatly [29,30]. Oxidative stress resulting from ROS is a known pathogenic factor in renal ischemia/reperfusion injury [31]. ROS inflict damage on lipids, proteins and DNAs [32–35]. In order to clarify the role of ROS in the DDR observed during recovery of ATP-depleted cells, we examined the effect of N-acetylcysteine (NAC), a general antioxidant. As shown in Fig. 5A (lane 4 vs. 3, lane 6 vs. 5), NAC suppressed the phosphorylation of ATM (Ser1981), Chk2 (Thr68) and p53 (Ser15) at 1 and 3 h of recovery following azide-induced ATP depletion. Surprisingly, γ H2AX level was not suppressed, but further induced by NAC (Fig. 5B). Immunofluorescence staining detected ~35%

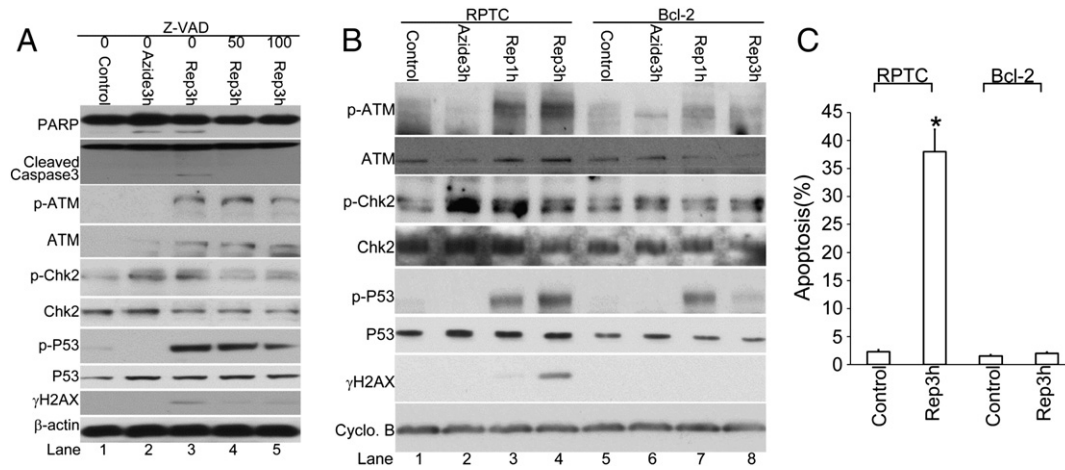


Fig. 4. Inhibition of DDR following azide treatment by Z-VAD and Bcl-2. (A) RPTC cells were left untreated (control) or treated with 10 mM sodium azide for 3 h followed by recovery of 0, 1, or 3 h in the presence or absence of 50 or 100 μM Z-VAD. Whole cell lysate was collected for immunoblot analysis of phosphorylated (Serine 1981) ATM, phosphorylated H2AX (γH2AX), PARP, cleaved Caspase3, phosphorylated (threonine 68) Chk2, total Chk2, phosphorylated (Serine 15) p53, total p53, and β-actin as a loading control. (B) Regular and Bcl-2-overexpressing RPTCs were left untreated (control) or treated with 10 mM sodium azide for 3 h followed by reperfusion of 0, 1, or 3 h. Whole cell lysate was collected for immunoblot analysis of phosphorylated (Serine 1981) ATM, phosphorylated H2AX (γH2AX), phosphorylated (threonine 68) Chk2, total Chk2, phosphorylated (Serine 15) p53, total p53, and Cyclophilin B as a loading control. (C) The percentage of apoptosis in RPTC and Bcl-2 cells after azide treatment and reperfusion was determined by counting the cells with typical apoptotic morphology.

cells with γH2AX nuclear foci during ATP depletion/recovery, which was increased to over 60% by NAC (Fig. 5C, D).

3.6. NAC increases apoptosis during recovery of ATP-depleted cells

The γH2AX increase by NAC during recovery of ATP-depleted RPTCs in above Fig. 5 was intriguing. We noticed that NAC increased apoptosis in this experiment (Fig. 6A). For quantification, we counted the cells with typical apoptotic morphology. As shown in Fig. 6B, 3 h of recovery of azide-treated cells induced ~40% apoptosis, which was further increased to ~60% by NAC. With this result, we considered the possibility that the γH2AX induction by NAC is secondary to the higher level of apoptosis and the associated DNA damage. In line with this possibility, the

caspase inhibitor Z-VAD diminished γH2AX expression in the presence of NAC (Fig. 6C). NAC treatment also decreased cell survival (Fig. 6D),

3.7. Inhibition of ATM increases apoptosis and γH2AX following ATP depletion and decreases cell survival

ATM is an early sensor in DDR. Depending on the cellular context, ATM may activate the signaling pathway of cell death or of DNA repair. To determine the role of ATM activation during recovery of ATP-depleted cells, we tested the effect of Ku55933, a specific ATM inhibitor. Ku55933 suppressed ATM phosphorylation during 1 and 3 h of recovery periods (Fig. 7C: lane 4 vs. 3, lane 6 vs. 5). To some extent, Ku55933 also suppressed Chk2 and p53 phosphorylation (Fig. 7C). Notably, Ku55933

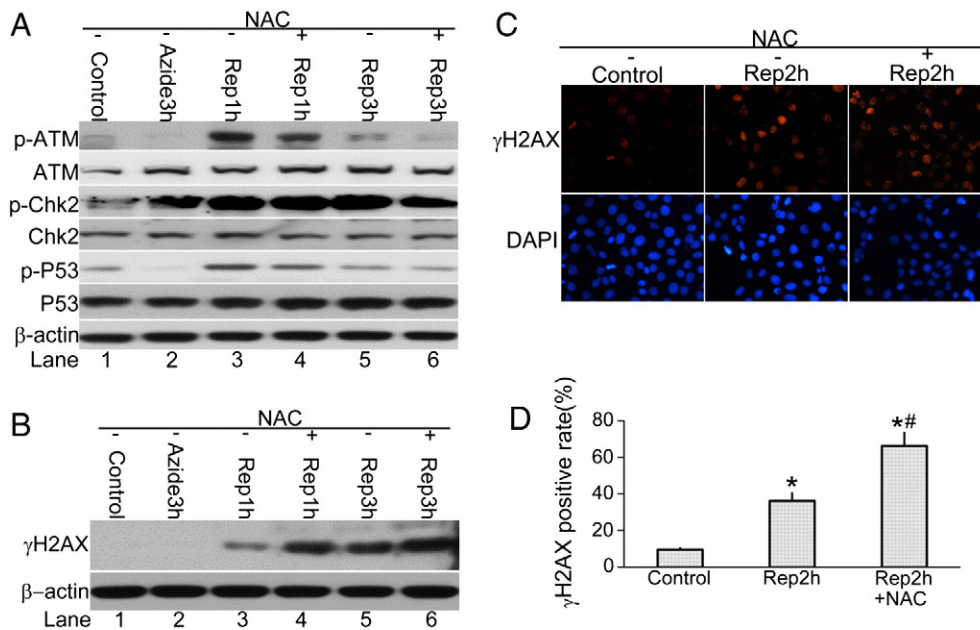


Fig. 5. NAC suppresses ATM activation following azide treatment. RPTC cells were left untreated (control) or treated with 10 mM sodium azide for 3 h followed by recovery in the presence or absence of 10 mM NAC. (A) Whole cell lysate was collected at the indicated recovery time for immunoblot analysis of phosphorylated (Serine 1981) ATM, phosphorylated (threonine 68) Chk2, total Chk2, phosphorylated (Serine 15) p53, total p53, and β-actin as a loading control. (B) Whole cell lysate was collected at the indicated recovery time for immunoblot analysis of phosphorylated H2AX (γH2AX), and β-actin as a loading control. (C) The cells were fixed at 2 h of recovery and subjected to immunofluorescence staining of γH2AX. (D) The cells with more than 3 γH2AX nuclear foci were counted to determine the percentage of γH2AX foci positive cells. *, $P < 0.05$ vs. control; #, $p < 0.05$ vs. Rep2h.

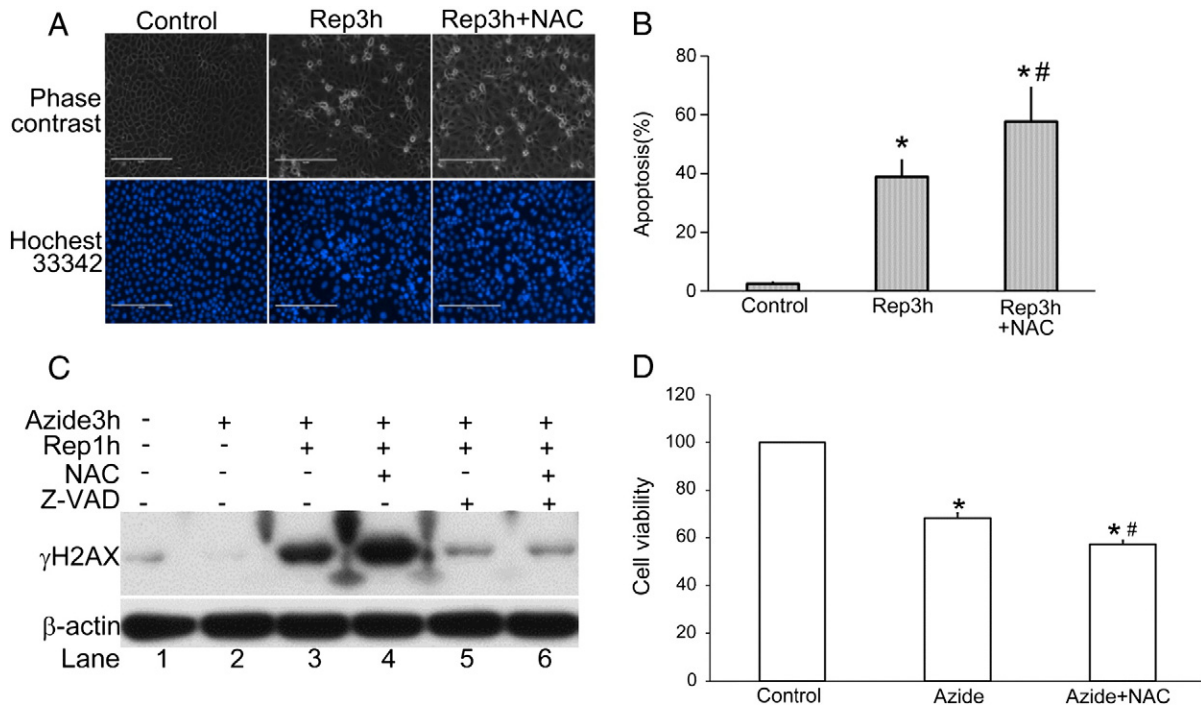


Fig. 6. NAC increases apoptosis, induces γ H2AX, and decreases cell survival following azide treatment. RPTCs were left untreated (control) or treated with 10 mM sodium azide for 3 h and then followed by recovery in the presence or absence of 10 mM NAC. (A, B) At 3 h of recovery, the cells were stained with Hoechst 33342 to record cellular morphology by phase contrast microscopy and nuclear morphology by fluorescence microscopy (A). (B) The percentage of apoptosis in each condition was determined by counting the cells with typical apoptotic morphology. (C) RPTCs were recovered for 0 or 1 h in the presence or absence of 10 mM NAC, 100 μ M Z-VAD, or 10 mM NAC + 100 μ M Z-VAD. Whole cell lysate was collected for immunoblot analysis of phosphorylated H2AX (γ H2AX) and β -actin (loading control). (D) RPTCs were left untreated (control) or treated with 10 mM sodium azide for 3 h and then followed by reperfusion of 3 h in the presence or absence of 10 mM NAC. After the treatment, the cells were recovered for 24 h in full culture medium to determine cell viability by MTT assay. Quantitative data are expressed as mean \pm SD ($n = 3$). *, $P < 0.05$ vs. control, #, $p < 0.05$ vs. azide group.

increased apoptosis from ~44% to ~66% (Fig. 7A, B). γ H2AX expression seemed to be increased by Ku55933 as well, so did γ H2AX nuclear foci formation (Fig. 7C–E). Finally, we analyzed the effect of Ku55933 on long-term cell survival. To this end, cell viability was analyzed by MTT assay 24 h after ATP-depletion treatment. As shown in Fig. 7F, Ku55933 decreased cell survival in a dose-dependent manner (Fig. 7F). Thus, the inhibition of ATM increased cell death and decreased cell viability in this in vitro model, suggesting that ATM activation plays a cytoprotective role for cell survival.

4. Discussion

Ischemia–reperfusion injury in organs and tissues leads to the development of ischemic diseases, including myocardial infarction, stroke in the brain and acute kidney injury. DNA damage and DDR-related proteins were reported to play important roles during ischemia–reperfusion injury in brain and heart [36–39]. However, the evidence of DDR in renal ischemia–reperfusion injury is sketchy, though the accumulation of 8-oxo-dG and apoptosis-associated DNA cleavage in renal tubular cells is known to occur in kidney tissues following ischemia–reperfusion [8–10]. In the present study, we have demonstrated the evidence of DDR in kidney tissues following ischemic–reperfusion injury in mice. Using the in vitro model of ‘chemical hypoxia’, we have further suggested the involvement of ATP depletion, oxidative stress, and apoptosis in the induction of DDR in renal tubular cells.

In general, the DDR shown in the in vitro model recapitulates the main features of that of in vivo renal ischemia/reperfusion. Especially, the phosphorylation of ATM, H2AX, Chk2 and p53 that are indicative of the activation of these proteins was all increased in both the in vitro and in vivo models. The expression of total proteins showed some differences between these two models. For example, total ATM was markedly induced during renal IRI, but it did not change significantly during

recovery or ‘reperfusion’ of ATP-depleted cells (Figs. 1, 2). In addition, total p53 accumulation was more evident in reperfused tissues than ATP-depleted cells, whereas p53 phosphorylation at ser-15 was more evident in the cells. These differences may result from the differences between the in vitro and in vivo models. Obviously, kidney tissues are much more complex as there are multiple cell types and during renal IRI, inflammatory cells also infiltrate into renal interstitium [1,2,40].

p53 plays a role in ischemic kidney injury [11,41,42]. P53 and Chk2 regulate the G2/M transition in response to stress and DNA damage as well [43,44]. Enhanced expression of p-ATM and p-Chk2 was reported in the post-ischemic kidneys and G2/M arrest induced by enhanced expression of p-Chk2 is associated with profibrotic cytokines production and kidney fibrosis progression after ischemia–reperfusion injury in kidney [45,46]. In this study, up regulated P53 and p-Chk2 both in ischemia-reperfused kidney cortex and ATP-depleted RPTC may participate in cellular repair and recovery by inducing cell cycle arrest, a possibility that needs to be tested in future study.

The signaling pathway activated during DDR is dependent on the type and extent of DNA damage. In our study, ATM showed an early phosphorylation or activation during the recovery of ATP-depleted cells, suggesting that ATM is a DNA damage sensor in this model. However, in the presence of NAC or Ku55933, while ATM activation was inhibited, γ H2AX increased. Since both NAC and Ku55933 increased apoptosis during ATP depletion/recovery, the observed γ H2AX induction is likely related to apoptosis-associated DNA damage. Under this condition, other DNA damage sensors such as ATR and DNA-PK may be activated to phosphorylate H2AX, a possibility that needs to be investigated in future studies.

In our study, the addition of glucose during azide treatment suppressed DDR. Glucose is the major substrate of glycolysis that promotes ATP production in RPTCs, especially under conditions of mitochondrial inhibition [47]. The suppressive effect of glucose on DDR in the

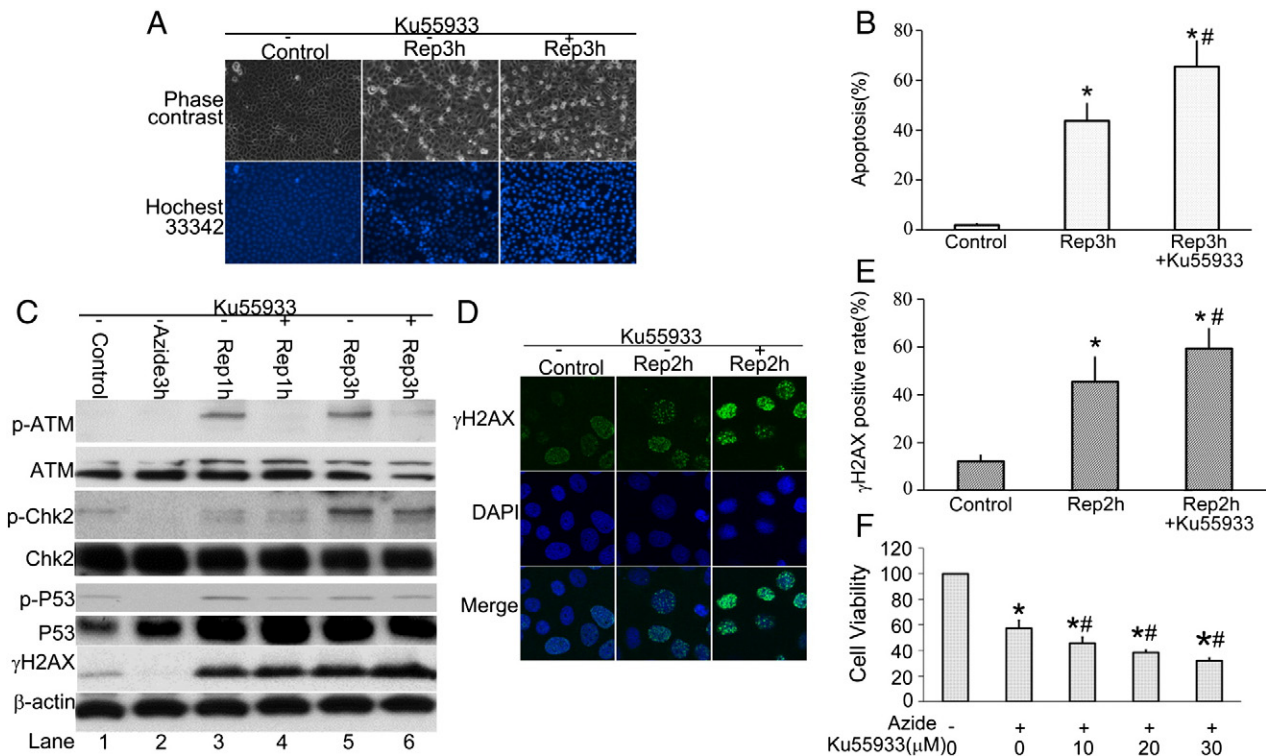


Fig. 7. Inhibition of ATM increases apoptosis and γ H2AX and decreases cell survival following azide treatment. RPTCs were left untreated (control) or treated with 10 mM sodium azide for 3 h and then followed by recovery of 1, 2 or 3 h in the presence or absence of 10 μ M Ku55933. (A, B) The cells were stained with Hoechst 33342 to record cellular morphology by phase contrast microscopy and nuclear morphology by fluorescence microscopy (A). The percentage of apoptosis in each condition was determined by counting the cells with typical apoptotic morphology (B). (C) Whole cell lysate was collected for immunoblot analysis of phosphorylated (Serine 1981) ATM, total ATM, phosphorylated (threonine 68) Chk2, total Chk2, phosphorylated (Serine 15) p53, total p53, phosphorylated H2AX (γ H2AX), total H2AX and β -actin (loading control). (D, E) RPTCs at 2 h of reperfusion were fixed for immunofluorescence of γ H2AX and nuclear staining with DAPI. The representative images of γ H2AX and DAPI staining were recorded (D) and the cells with more than 3 γ H2AX nuclear foci were counted to determine the percentage of γ H2AX positive cells (E). (F) After the treatment, the cells were recovered for 24 h in full culture medium to determine cell viability by MTT assay. Quantitative data are expressed as mean \pm SD (n = 3). *, P < 0.05 vs. control, #, p < 0.05 vs. azide group.

'chemical hypoxia' model indicates that the DDR is a result of ATP-depletion-triggered cell injury. This is not surprising because ATP depletion is largely responsible for the initiation of cell injury processes in this model, culminating in mitochondrial damage and ultimate cell death by apoptosis [17,26]. In this regard, our results also support a role of apoptosis in DDR in the ATP-depletion/recovery model. The work from us and others has demonstrated that renal tubular cells undergo apoptosis during ischemia–reperfusion in vivo and ATP-depletion in vitro via the intrinsic pathway mediated by mitochondrial injury [24,47]. In this apoptotic pathway, the activation of Bax and Bak leads to mitochondrial outer membrane permeabilization and the release of apoptotic factors including cytochrome c, which further activates caspases for the development of apoptosis. Bcl-2 antagonizes Bax and Bak to prevent mitochondrial permeabilization and inhibit apoptosis. In the present study, DDR was suppressed by the pan-caspase inhibitor Z-VAD and Bcl-2, supporting the involvement of apoptosis in the DDR. Apoptosis is often associated with internucleosomal DNA cleavage, which occurs in kidney tissues during renal ischemia–reperfusion [10]. Thus, the DDR observed in the present study is partly attributable to apoptosis-associated DNA damage.

Although both Z-VAD and Bcl-2 blocked apoptosis in our study, the effect of Z-VAD on DDR was less than that of Bcl-2 (Fig. 4). This observation suggests the presence of other mechanisms of DDR induction, in addition to apoptosis. The primary action of Bcl-2 is the protection of mitochondria, resulting in inhibition of caspase activation and apoptosis. Based on this consideration, our results support an apoptosis-independent role of mitochondrial damage in triggering DDR, although the underlying mechanism is currently unclear. It is suggested that there are two phases of DDR activation in the ATP-depletion/recovery model. The initial phase of DDR activation is indicated by the ATM

activation, which is mainly due to mitochondrial injury, resulting in a mild γ H2AX induction. The inhibitory effect of NAC suggests that oxidative stress may also contribute to the early activation of ATM, probably as a result of mitochondrial injury. The ATM activation in this study leads to the downstream phosphorylation of Chk2 and p53. Some reports show that NAC protects against drug and oxidative stress-induced apoptosis [48–53]. However, NAC has also been shown to induce apoptosis in multiple types of cells by increasing the pro-apoptotic Bax gene expression, or by inhibiting expression of anti-apoptotic proteins Bcl-2, or via the ER stress response-signaling pathway [29,54,55]. Our studies show that NAC treatment enhances apoptosis and decreased cell survival following ATP-depletion injury in RPTC (Fig. 6). NAC may exert this effect partially by inhibiting ATM, a surviving signaling pathway in this model, but further studies need to delineate the finding. The second phase of DDR is apoptosis or caspase activation related, and is mainly indicated by the massive induction of γ H2AX. As discussed above, apoptosis-associated DDR seems less dependent on ATM, because Ku55933 completely blocked ATM activation yet increase γ H2AX induction and apoptosis. According to our results, the initial phase of DDR mediated by ATM after mitochondrial injury may be cytoprotective, while the second phase of DDR indicated by massive γ H2AX induction is mainly an indication of extensive DNA damage in apoptosis. ATM is known to activate the mechanism of DNA repair in DDR, which may account for the cytoprotective effect of ATM in our study. In addition, ATM may be involved in the regulation of antioxidant defense [56]. In support of this possibility, ATM mutation or deficient were reported to affect cellular antioxidant status, including decreased amounts of antioxidant molecules and glutathione biosynthesis in A–T cells and increased concentrations of superoxide anions in the cerebella in ATM $-/-$ mice [57–59].

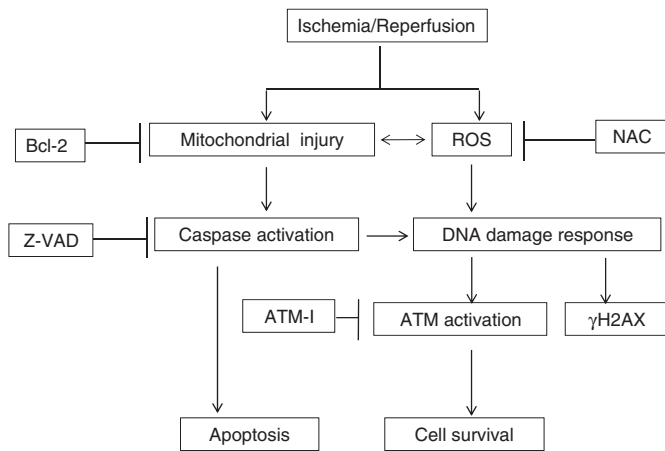


Fig. 8. A schematic summary of DDR in cell death and survival following ischemia–reperfusion.

In conclusion, this study has demonstrated the occurrence of DDR during renal ischemia–reperfusion *in vivo* and ATP-depletion injury *in vitro*. The DDR may consist of two phases (Fig. 8). The first phase of DDR is mediated by ATM and depends on mitochondrial injury, whereas the second phase is indicated by γ H2AX induction and is consequent to tubular cell apoptosis. ATM-mediated DDR may have a cytoprotective role. Modulation of the DDR may therefore offer a new strategy for kidney protection during renal ischemia–reperfusion.

References

- J.V. Bonventre, L. Yang, Cellular pathophysiology of ischemic acute kidney injury, *J. Clin. Invest.* 121 (2011) 4210–4221.
- A.A. Sharfuddin, B.A. Molitoris, Pathophysiology of ischemic acute kidney injury, *Nat. Rev. Nephrol.* 7 (2011) 189–200.
- L.S. Chawla, P.L. Kimmel, Acute kidney injury and chronic kidney disease: an integrated clinical syndrome, *Kidney Int.* 82 (2012) 516–524.
- M.A. Venkatachalam, K.A. Griffin, R. Lan, H. Geng, P. Saikumar, et al., Acute kidney injury: a springboard for progression in chronic kidney disease, *Am. J. Physiol. Ren. Physiol.* 298 (2010) F1078–F1094.
- C.H. McGowan, P. Russell, The DNA damage response: sensing and signaling, *Curr. Opin. Cell Biol.* 16 (2004) 629–633.
- R.L. Flynn, L. Zou, ATR: a master conductor of cellular responses to DNA replication stress, *Trends Biochem. Sci.* 36 (2011) 133–140.
- A. Sancar, L.A. Lindsey-Boltz, K. Unsal-Kacmaz, S. Linn, Molecular mechanisms of mammalian DNA repair and the DNA damage checkpoints, *Annu. Rev. Biochem.* 73 (2004) 39–85.
- K. Tsuruya, M. Furuichi, Y. Tominaga, M. Shinozaki, M. Tokumoto, et al., Accumulation of 8-oxoguanine in the cellular DNA and the alteration of the OGG1 expression during ischemia–reperfusion injury in the rat kidney, *DNA Repair (Amst)* 2 (2003) 211–229.
- T. Yoshida, A. Shimizu, Y. Masuda, A. Mii, E. Fujita, et al., Caspase-3-independent internucleosomal DNA fragmentation in ischemic acute kidney injury, *Nephron Exp. Nephrol.* 120 (2012) e103–e113.
- M. Schumer, M.C. Colombel, I.S. Sawczuk, G. Gobe, J. Connor, et al., Morphologic, biochemical, and molecular evidence of apoptosis during the reperfusion phase after brief periods of renal ischemia, *Am. J. Pathol.* 140 (1992) 831–838.
- T. Fujino, S. Muhib, N. Sato, N. Hasebe, Silencing of p53 RNA through transarterial delivery ameliorates renal tubular injury and down-regulates GSK-3 β expression after ischemia–reperfusion injury, *Am. J. Physiol. Ren. Physiol.* 305 (2013) F1617–AAA1627.
- K.J. Kelly, Z. Plotkin, S.L. Vulgamott, P.C. Dagher, P53 mediates the apoptotic response to GTP depletion after renal ischemia–reperfusion: protective role of a p53 inhibitor, *J. Am. Soc. Nephrol.* 14 (2003) 128–138.
- N. Pabla, Z. Ma, M.A. McIlhatton, R. Fisher, Z. Dong, hMSH2 recruits ATR to DNA damage sites for activation during DNA damage-induced apoptosis, *J. Biol. Chem.* 286 (2011) 10411–10418.
- N. Pabla, S. Huang, Q.S. Mi, R. Daniel, Z. Dong, ATR-Chk2 signaling in p53 activation and DNA damage response during cisplatin-induced apoptosis, *J. Biol. Chem.* 283 (2008) 6572–6583.
- M. Jiang, Q. Wei, J. Wang, Q. Du, J. Yu, et al., Regulation of PUMA- α by p53 in cisplatin-induced renal cell apoptosis, *Oncogene* 25 (2006) 4056–4066.
- Q. Wei, Z. Dong, Mouse model of ischemic acute kidney injury: technical notes and tricks, *Am. J. Physiol.* 303 (2012) F1487–F1494.
- C. Brooks, Q. Wei, S.G. Cho, Z. Dong, Regulation of mitochondrial dynamics in acute kidney injury in cell culture and rodent models, *J. Clin. Invest.* 119 (2009) 1275–1285.
- P. Saikumar, Z. Dong, Y. Patel, K. Hall, U. Hopfer, et al., Role of hypoxia-induced Bax translocation and cytochrome c release in reoxygenation injury, *Oncogene* 17 (1998) 3401–3415.
- T. Uziel, Y. Lerenthal, L. Moyal, Y. Andegeko, L. Mittelman, et al., Requirement of the MRN complex for ATM activation by DNA damage, *EMBO J.* 22 (2003) 5612–5621.
- A. Jazayeri, A. Balestrini, E. Garner, J.E. Haber, V. Costanzo, Mre11-Rad50-Nbs1-dependent processing of DNA breaks generates oligonucleotides that stimulate ATM activity, *EMBO J.* 27 (2008) 1953–1962.
- Y. Shiloh, Y. Ziv, The ATM protein kinase: regulating the cellular response to genotoxic stress, and more, *Nat. Rev. Mol. Cell Biol.* 14 (2013) 197–210.
- A. Sharma, K. Singh, A. Almasan, Histone H2AX phosphorylation: a marker for DNA damage, *Methods Mol. Biol.* 920 (2012) 613–626.
- T. Tanaka, D. Halicka, F. Traganos, Z. Darzynkiewicz, Cytometric analysis of DNA damage: phosphorylation of histone H2AX as a marker of DNA double-strand breaks (DSBs), *Methods Mol. Biol.* 523 (2009) 161–168.
- Q. Wei, G. Dong, J.K. Chen, G. Ramesh, Z. Dong, Bax and Bak have critical roles in ischemic acute kidney injury in global and proximal tubule-specific knockout mouse models, *Kidney Int.* 84 (2013) 138–148.
- M. Jiang, Q. Wei, G. Dong, M. Komatsu, Y. Su, et al., Autophagy in proximal tubules protects against acute kidney injury, *Kidney Int.* 82 (2012) 1271–1283.
- Z. Dong, J.Z. Wang, F. Yu, M.A. Venkatachalam, Apoptosis-resistance of hypoxic cells: multiple factors involved and a role for IAP-2, *Am. J. Pathol.* 163 (2003) 663–671.
- B. Halliwell, J.M. Gutteridge, Role of free radicals and catalytic metal ions in human disease: an overview, *Methods Enzymol.* 186 (1990) 1–85.
- J. Boonstra, J.A. Post, Molecular events associated with reactive oxygen species and cell cycle progression in mammalian cells, *Gene* 337 (2004) 1–13.
- S. Qanungo, M. Wang, A.L. Nieminen, N-Acetyl-L-cysteine enhances apoptosis through inhibition of nuclear factor- κ B in hypoxic murine embryonic fibroblasts, *J. Biol. Chem.* 279 (2004) 50455–50464.
- A. Roy, A. Ganguly, S. BoseDasgupta, B.B. Das, C. Pal, et al., Mitochondria-dependent reactive oxygen species-mediated programmed cell death induced by 3,3'-diindolylmethane through inhibition of FOF1-ATP synthase in unicellular protozoan parasite *Leishmania donovani*, *Mol. Pharmacol.* 74 (2008) 1292–1307.
- A.G. Basnakian, G.P. Kaushal, S.V. Shah, Apoptotic pathways of oxidative damage to renal tubular epithelial cells, *Antioxid. Redox Signal.* 4 (2002) 915–924.
- E. Noiri, A. Nakao, K. Uchida, H. Tsukahara, M. Ohno, et al., Oxidative and nitrosative stress in acute renal ischemia, *Am. J. Physiol. Ren. Physiol.* 281 (2001) F948–F957.
- A. Barzilai, K. Yamamoto, DNA damage responses to oxidative stress, *DNA Repair (Amst)* 3 (2004) 1109–1115.
- P.D. Ray, B.W. Huang, Y. Tsuji, Reactive oxygen species (ROS) homeostasis and redox regulation in cellular signaling, *Cell. Signal.* 24 (2012) 981–990.
- A. Srinivasan, H.J. Lehmler, L.W. Robertson, G. Ludewig, Production of DNA strand breaks *in vitro* and reactive oxygen species *in vitro* and in HL-60 cells by PCB metabolites, *Toxicol. Sci.* 60 (2001) 92–102.
- P.K. Liu, C.Y. Hsu, M. Dizdaroglu, R.A. Floyd, Y.W. Kow, et al., Damage, repair, and mutagenesis in nuclear genes after mouse forebrain ischemia–reperfusion, *J. Neurosci.* 16 (1996) 6795–6806.
- G.A. Cordis, D. Bagchi, W. Riedel, S.J. Stohs, D.K. Das, Implication of DNA damage during reperfusion of ischemic myocardium, *Ann. N. Y. Acad. Sci.* 793 (1996) 427–430.
- J. Cui, E.H. Holmes, T.G. Greene, P.K. Liu, Oxidative DNA damage precedes DNA fragmentation after experimental stroke in rat brain, *FASEB J.* 14 (2000) 955–967.
- P.C. Shukla, K.K. Singh, A. Quan, M. Al-Omran, H. Teoh, et al., BRCA1 is an essential regulator of heart function and survival following myocardial infarction, *Nat. Commun.* 2 (2011) 593.
- G.R. Kinsey, R. Sharma, M.D. Okusa, Regulatory T cells in AKI, *J. Am. Soc. Nephrol.* 24 (2013) 1720–1726.
- D. Zhang, Y. Liu, Q. Wei, Y. Huo, K. Liu, F. Liu, Z. Dong, Tubular p53 regulates multiple genes to mediate acute kidney injury, *J. Am. Soc. Nephrol.* (2014) (in press) (Epub ahead of print).
- B.A. Molitoris, P.C. Dagher, R.M. Sandoval, S.B. Campos, H. Ashush, et al., siRNA targeted to p53 attenuates ischemic and cisplatin-induced acute kidney injury, *J. Am. Soc. Nephrol.* 20 (2009) 1754–1764.
- W.R. Taylor, G.R. Stark, Regulation of the G2/M transition by p53, *Oncogene* 20 (2001) 1803–1815.
- S. Matsuo, M. Huang, S.J. Elledge, Linkage of ATM to cell cycle regulation by the Chk2 protein kinase, *Science* 282 (1998) 1893–1897.
- H.S. Jang, S.J. Han, J.I. Kim, S. Lee, J.H. Lipschutz, et al., Activation of ERK accelerates repair of renal tubular epithelial cells, whereas it inhibits progression of fibrosis following ischemia/reperfusion injury, *Biochim. Biophys. Acta* 1832 (2013) 1998–2008.
- L. Yang, T.Y. Besschetnova, C.R. Brooks, J.V. Shah, J.V. Bonventre, Epithelial cell cycle arrest in G2/M mediates kidney fibrosis after injury, *Nat. Med.* 16 (2010) 535–543 (531 pp. following 143).
- P. Saikumar, Z. Dong, J.M. Weinberg, M.A. Venkatachalam, Mechanisms of cell death in hypoxia/reoxygenation injury, *Oncogene* 17 (1998) 3341–3349.
- X. Gong, G. Celsi, K. Carlsson, S. Norgren, M. Chen, N-acetylcysteine amide protects renal proximal tubular epithelial cells against iohexol-induced apoptosis by blocking p38 MAPK and iNOS signaling, *Am. J. Nephrol.* 31 (2010) 178–188.
- L. Sun, L. Gu, S. Wang, J. Yuan, H. Yang, et al., N-acetylcysteine protects against apoptosis through modulation of group I metabotropic glutamate receptor activity, *PLoS One* 7 (2012) e32503.
- H.M. Jin, D.C. Zhou, H.F. Gu, Q.Y. Qiao, S.K. Fu, et al., Antioxidant N-acetylcysteine protects pancreatic beta-cells against aldosterone-induced oxidative stress and apoptosis in female db/db mice and insulin-producing MIN6 cells, *Endocrinology* 154 (2013) 4068–4077.

- [51] J.H. Kim, S.S. Lee, M.H. Jung, H.D. Yeo, H.J. Kim, et al., N-acetylcysteine attenuates glycerol-induced acute kidney injury by regulating MAPKs and Bcl-2 family proteins, *Nephrol. Dial. Transplant.* 25 (2010) 1435–1443.
- [52] Y.L. Ji, H. Wang, C. Zhang, Y. Zhang, M. Zhao, et al., N-acetylcysteine protects against cadmium-induced germ cell apoptosis by inhibiting endoplasmic reticulum stress in testes, *Asian J. Androl.* 15 (2013) 290–296.
- [53] W.K. Low, L. Sun, M.G. Tan, A.W. Chua, D.Y. Wang, L-N-Acetylcysteine protects against radiation-induced apoptosis in a cochlear cell line, *Acta Otolaryngol.* 128 (2008) 440–445.
- [54] D. Guan, Y. Xu, M. Yang, H. Wang, X. Wang, et al., N-acetyl cysteine and penicillamine induce apoptosis via the ER stress response-signaling pathway, *Mol. Carcinog.* 49 (2010) 68–74.
- [55] M. Rieber, M.S. Rieber, N-Acetylcysteine enhances UV-mediated caspase-3 activation, fragmentation of E2F-4, and apoptosis in human C8161 melanoma: inhibition by ectopic Bcl-2 expression, *Biochem. Pharmacol.* 65 (2003) 1593–1601.
- [56] C. Cosentino, D. Grieco, V. Costanzo, ATM activates the pentose phosphate pathway promoting anti-oxidant defence and DNA repair, *EMBO J.* 30 (2011) 546–555.
- [57] S. Ditch, T.T. Paull, The ATM protein kinase and cellular redox signaling: beyond the DNA damage response, *Trends Biochem. Sci.* 37 (2012) 15–22.
- [58] X. Kuang, M. Yan, J.M. Ajmo, V.L. Scofield, G. Stoica, et al., Activation of AMP-activated protein kinase in cerebella of *Atm*^{-/-} mice is attributable to accumulation of reactive oxygen species, *Biochem. Biophys. Res. Commun.* 418 (2012) 267–272.
- [59] A. Kamsler, D. Daily, A. Hochman, N. Stern, Y. Shiloh, et al., Increased oxidative stress in ataxia telangiectasia evidenced by alterations in redox state of brains from *Atm*-deficient mice, *Cancer Res.* 61 (2001) 1849–1854.